



ON THE DESIGN OF MODAL ACTUATORS AND SENSORS

M. I. FRISWELL

*Department of Mechanical Engineering, University of Wales Swansea, Swansea SA2 8PP, Wales.
E-mail: m.i.friswell@swansea.ac.uk*

(Received 9 March 2000, and in final form 31 July 2000)

Modal actuators and sensors may be used to excite or measure either single modes or combinations of modes. In beam structures they may be implemented using either discrete transducers or continuous, distributed transducers. This paper determines the transducer gains to obtain given modal responses. For discrete transducers, when there are more transducers than modes of interest, this generally results an underdetermined problem. Side constraints, either by choosing a subset of transducers, or ensuring orthogonality to higher modes, make use of this redundancy. For distributed transducers this paper introduces the idea of approximating the width of the transducer using the underlying finite element model shape functions. The transducers may then be designed using a discrete model, and the shape recovered by using the shape functions. The side constraint of minimizing the curvature of the transducer shape is introduced to ensure that the resulting shape is as simple as possible. A clamped–clamped beam example is used to demonstrate the effectiveness of the proposed methods, and also to demonstrate the errors introduced for non-proportionally damped structures.

© 2001 Academic Press

1. INTRODUCTION

The idea of using modal sensors and actuators for beam- and plate-type structures has been a subject of intense interest for many years. Using modal sensors in active control reduces problems of spillover, where high-frequency unmodelled modes affect the stability of the closed-loop system. The sensors and actuators may be discrete or continuous. For example, a modal sensor for a beam-type structure may be obtained by varying the sensor width along the length of the beam. If the sensor covers the whole beam the shape of the sensor may be derived using the mode shape orthogonality property. Lee and Moon [1] and Clark and Burke [2] have provided good summaries of the state of the art in this area. Tanaka *et al.* [3] placed a number of sensor patches on the structure to measure the response at a number of modes. They used sensors covering the whole beam, and based their shape on combinations of the beam mode shapes. Zhuang and Baras [4] discretized the sensor shape using piecewise constant functions and used dynamic programming to optimize an energy function that described the level of vibration in a composite beam. Hsu *et al.* [5] designed modal sensors and actuators for laminated beams. Friswell [6] considered modal sensors that cover only part of the beam, and segmented modal sensors for multiple modes. He also considered the effect of geometric tolerances during manufacture on the quality of the sensors. Gawronski [7] considered the case of discrete sensors and actuators, and from these derived continuous actuator widths. This paper extends the approach of Gawronski, by considering what extra side constraints could be imposed when the number of actuators or sensors is greater than the modes of interest (as may often be the case in a smart structure application). Also considered is how the continuous actuators and sensors may be derived

from the discrete approximation in a consistent way. The latter uses the underlying shape functions of the finite element model to approximate the transducer shape. The proposed approaches are demonstrated on a beam structure.

2. GENERAL MODAL ACTUATORS AND SENSORS FOR DISCRETE MODELS

Discrete models will be considered first. These models are generally determined from a finite element analysis, and are of the form

$$\mathbf{M}\ddot{\mathbf{q}} + \mathbf{D}\dot{\mathbf{q}} + \mathbf{K}\mathbf{q} = \mathbf{B}\mathbf{u}, \quad \mathbf{y} = \mathbf{C}_q\mathbf{q} + \mathbf{C}_\dot{q}\dot{\mathbf{q}}, \quad (1)$$

where \mathbf{M} , \mathbf{D} and \mathbf{K} are the mass, damping and stiffness matrices based on the degrees of freedom, \mathbf{q} . In practice, the equations of motion will often be reduced, for example by eliminating rotational degrees of freedom. The inputs to the structure, \mathbf{u} , are applied via a matrix \mathbf{B} which determines the location and gain of the actuators. Similarly the outputs, \mathbf{y} , are obtained via the output matrices \mathbf{C}_q and $\mathbf{C}_\dot{q}$ which are determined by the sensor location and gains and also whether displacement or velocity is measured. Proportional damping will be assumed so that the mode shapes of equation (1) are real, and equal to the mode shapes of the undamped system. For light damping this approximation will introduce small errors, but these errors will be considered later. The mode shapes, Φ , are assumed to be normalized arbitrarily so that the modal mass is

$$\Phi^T \mathbf{M} \Phi = \mathbf{M}_m. \quad (2)$$

Applying the transformation to modal co-ordinates, $\mathbf{q} = \Phi\mathbf{p}$, to equation (1), gives

$$\ddot{\mathbf{p}} + 2\mathbf{Z}\mathbf{Z}\mathbf{Z}\dot{\mathbf{p}} + \mathbf{Z}^2\mathbf{p} = \mathbf{M}_m^{-1}\Phi^T\mathbf{B}\mathbf{u} = \mathbf{B}_m\mathbf{u}, \quad \mathbf{y} = \mathbf{C}_q\Phi\mathbf{p} + \mathbf{C}_\dot{q}\Phi\dot{\mathbf{p}} = \mathbf{C}_p\mathbf{p} + \mathbf{C}_\dot{p}\dot{\mathbf{p}}, \quad (3)$$

where $\mathbf{Z} = \text{diag}[\omega_1, \omega_2, \dots, \omega_n]$ is a diagonal matrix of the natural frequencies, and $\mathbf{Z} = \text{diag}[\zeta_1, \zeta_2, \dots, \zeta_n]$ are the modal damping ratios. The input and output matrices have been transformed to their modal equivalents, defined in equation (3).

The question addressed by Gawronski [7] was the determination of the actuator matrix, \mathbf{B} , given the required modal input gain matrix, \mathbf{B}_m . Clearly, the modes must be scaled in some consistent manner, since otherwise for a particular set of input gains the modal input gain matrix will change depending on the mode scaling. This is particularly important when more than one mode is excited. From equation (3)

$$\mathbf{B}_m = \mathbf{M}_m^{-1}\Phi^T\mathbf{B} = \mathbf{R}\mathbf{B}, \quad (4)$$

where $\mathbf{R} = \mathbf{M}_m^{-1}\Phi^T$. Gawronski suggested that the pseudo inverse of \mathbf{R} , obtained via the singular-value decomposition (SVD), is used to compute \mathbf{B} as

$$\mathbf{B} = \mathbf{R}^+\mathbf{B}_m. \quad (5)$$

The question addressed in this paper is whether the pseudo inverse based on the SVD is the best solution. Given \mathbf{B}_m and \mathbf{R} , and assuming there are more actuators than modes of interest, means that equation (4) is underdetermined. The SVD solution gives the minimum norm solution, but the actual solution will depend on the scaling of the modes, which is arbitrary. Gawronski gave no guidelines for the choice of scaling, but clearly this is important.

The derivation of a modal sensor is almost identical. If a modal displacement sensor is required then, from equation (3), upon assuming the modal output matrix C_p is given and $C_p = \mathbf{0}$, then

$$C_q \Phi = C_p \quad (6)$$

and the discrete sensor gain matrix C_q may be obtained from the pseudo inverse, or the alternatives described below. If the modes are mass normalized the procedure is exactly the same as that for the actuators. The procedure for velocity sensors is very similar. Of course, just as controllability and observability cannot be treated in isolation [8], so modal actuators and sensors cannot be treated in isolation. Gawronski [7] outlined a procedure to weight the modal input and output gain matrices to give the required frequency response function magnitude, and this will not be considered further here. The ultimate situation is to have a modal self sensing actuator [9], in which case the input and output matrices are coupled, but incorporating this natural coupling into the proposed procedures is relatively simple. Since the procedure to derive the sensor gains is so similar to deriving the actuator gains, only the latter will be considered in detail.

3. SIDE CONSTRAINTS FOR ACTUATOR GAINS

If there are more actuators than modes of interest, then equation (4) is underdetermined, and extra constraints need to be imposed. The Moore–Penrose pseudo inverse, conveniently implemented by using the SVD, minimizes the sum of squares of the actuator gains. If all the actuators are of the same type, then this sum of squares of the actuator gains relates directly to the energy required to excite the mode. Thus, the minimum norm solution may be interpreted as a minimum energy solution. However, this will not be the case if the rotational degrees of freedom are retained, and there is a mixture of translational and rotational actuators.

Three alternative constraints will be considered here. The first is to select only a minimum subset of the actuators to have non-zero gains. Clearly, this is not appropriate for distributed sensors, although it could be used to force only the translational sensors to be non-zero, rather than reduce the model. The choice of non-zero sensors may be made *a priori* from physical understanding, as in the case of eliminating rotational degrees of freedom, or automatically via some optimization scheme. Automatic selection is similar to subset selection schemes for identification [10, 11] and will not be pursued further.

The second possibility is make the actuator orthogonal to higher modes (i.e., modes assumed to be of no interest). This implies that neglected modes might be important. On the assumption that the mass matrix is available, the solution is immediately computed as

$$\mathbf{B} = \mathbf{M}\Phi\mathbf{B}_m. \quad (7)$$

Similar approaches have long been applied in vibration control [12] and reduce spillover from the higher modes. Indeed an equivalent approach has been standard for distributed modal transducers for beam structures.

The final constraint is to ensure that the curvature of the distributed actuator is a minimum. This constraint is difficult to apply to discrete actuators, and so further consideration is delayed until later.

4. A BEAM EXAMPLE

The clamped-clamped beam example similar to that used by Gawronski [7] will be used here. The steel beam is 1.5 m long with cross-section 20 mm \times 5 mm, and bending in the more flexible plane is modelled by using 15 finite elements. Only the first nine modes are considered important and damping is assumed to be 1% in all modes. Table 1 gives the first 12 natural frequencies for the beam. The output will be measured at node 7 for actuator design; Gawronski took the output to be the sum of the lateral displacements, but unfortunately all the even modes (including the second) are unobservable to this output.

An actuator is designed such that only the second of the first nine modes is excited, and the maximum of the receptance (based on the displacement of node 6 as the output) is 0.01 m/N. Figure 1 shows the results based on applying the pseudo inverse for all degrees of freedom. The upper plot shows the translational actuator gains and the lower plot shows the receptance, clearly demonstrating that the specification has been met. Of course there are also rotational actuator gains that are not shown. Figure 2 shows the translational actuator gains when the rotational actuator gains are constrained to be zero. The gains were obtained using the pseudo inverse, but by zeroing the rows of \mathbf{R} corresponding to the

TABLE 1
The first 12 natural frequencies of the clamped-clamped beam

Mode No.	Natural Frequency (Hz)	Mode No.	Natural Frequency (Hz)
1	11.815	7	294.33
2	32.569	8	378.97
3	63.858	9	474.95
4	105.60	10	582.69
5	157.84	11	702.61
6	220.70	12	834.86

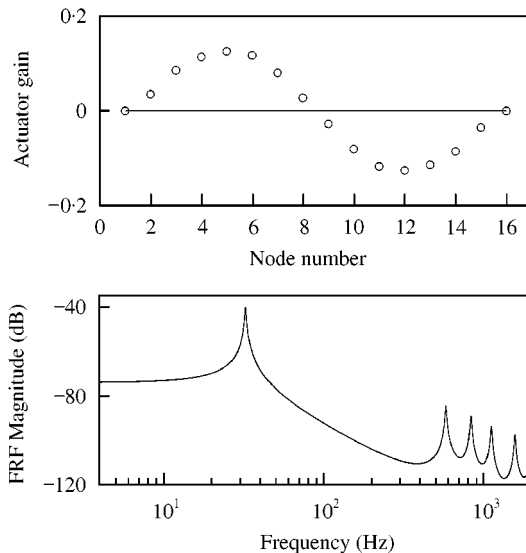


Figure 1. The Actuator gains and receptance designed to excite the second mode using the pseudo inverse approach.

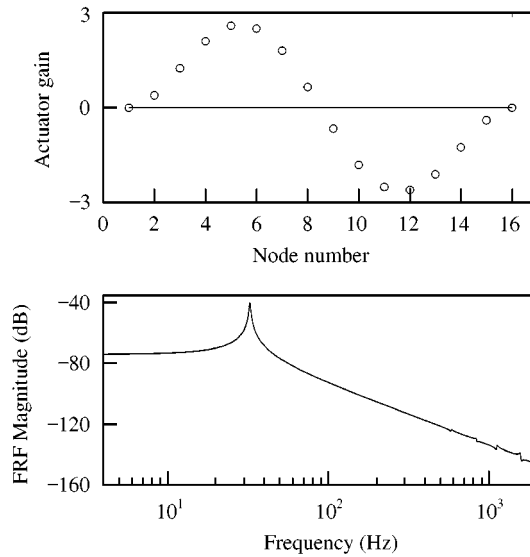


Figure 2. As Figure 1 but for only the translational degrees of freedom.

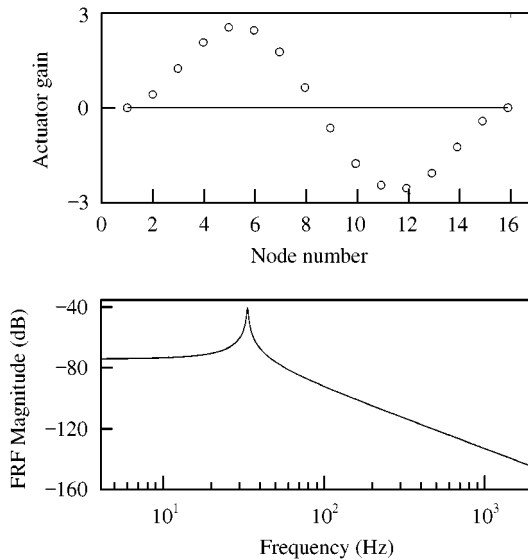


Figure 3. The actuator gains and receptance designed to excite the second mode and to be orthogonal to the higher modes.

rotational degrees of freedom. The gains are significantly different in magnitude, and the shape of the curve is different near the ends of the beam. The receptance shows that this actuator is more orthogonal to the higher modes than the first case. Figure 3 shows the case where the actuator gains are chosen to be orthogonal to the higher modes, and produces similar actuator gains to the second case, where the gain corresponding to the rotational degrees of freedom was zeroed.

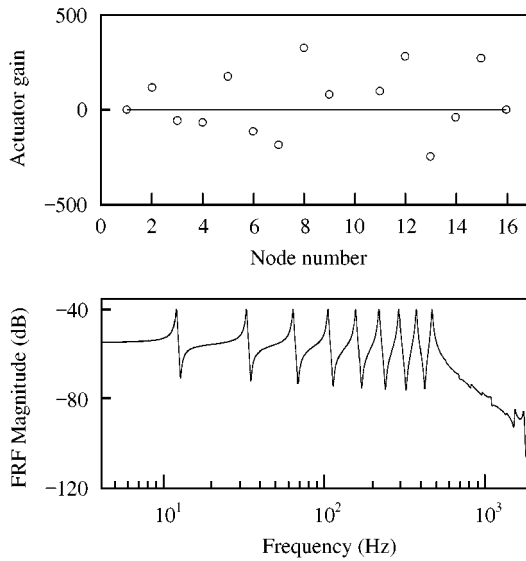


Figure 4. The actuator gains and receptance designed to excite the first nine modes using the pseudo inverse approach for the translational degrees of freedom only.

Suppose now that all of the first nine modes need to be excited, so that the receptance reaches a maximum of 0.01 m/N at every mode. Figure 4 shows the results obtained by using the pseudo inverse, when the rotational gains are zero. Clearly, the receptance fulfils the requirements, although the actuator gains do not correspond to a simple shape.

5. APPROXIMATING TRANSDUCER WIDTHS USING SHAPE FUNCTIONS

Thus far a discrete model of the structure has been assumed, which has produced modal actuators and sensors by varying the gain to the discrete transducers. An alternative to a large number of discrete transducers is to employ distributed actuators and sensors, often implemented using piezoelectric materials. Most papers concerned with distributed transducers are concerned with beams where the partial differential equations of motion may be solved to derive the continuous mode shapes. Here a different approach is taken and the shape functions of the underlying finite element model are used to approximate the width of the piezoelectric material. In this way, modal transducers may be designed for arbitrary beam-type structures. Also, by using the side constraint from section 3 that not all degrees of freedom are forced or sensed, modal transducers than only cover part of a structure may be designed. Most of the development will concern sensors, although actuators may be dealt with in a similar way, as shown at the end of this section.

Suppose a single polyvinylidene fluoride (PVDF) film sensor is placed on the beam with a shape defined by a variable width $f(\xi)$, where ξ denotes the length along the beam element. Incorporated into $f(\xi)$ is both the physical width of the sensor, and also the polarization profile of the material. The central feature of the proposed method is to approximate this width using the shape functions of the underlying finite element model. For an

Euler–Bernoulli beam these shape functions, for element number e , are

$$\begin{aligned}
 N_{e1}(\xi) &= \left(1 - 3\frac{\xi^2}{\ell_e^2} + 2\frac{\xi^3}{\ell_e^3}\right), & N_{e2}(\xi) &= \ell_e \left(\frac{\xi}{\ell_e} - 2\frac{\xi^2}{\ell_e^2} + \frac{\xi^3}{\ell_e^3}\right), \\
 N_{e3}(\xi) &= \left(3\frac{\xi^2}{\ell_e^2} - 2\frac{\xi^3}{\ell_e^3}\right), & N_{e4}(\xi) &= \ell_e \left(-\frac{\xi^2}{\ell_e^2} + \frac{\xi^3}{\ell_e^3}\right),
 \end{aligned}
 \tag{8}$$

where ℓ_e is the length of the element. Thus, the sensor width within element number e is approximated as

$$f_e(\xi) = [N_{e1}(\xi) N_{e2}(\xi) N_{e3}(\xi) N_{e4}(\xi)] \begin{Bmatrix} f_{e1} \\ f_{e2} \\ f_{e3} \\ f_{e4} \end{Bmatrix}
 \tag{9}$$

where the constants f_{ei} must be determined. This approximation has the advantage that the width and slope of the sensor are continuous at the nodes of the finite element model. The output (voltage or charge) from the part of the sensor with element number e is

$$y_e(t) = K_s \int_0^{\ell_e} f_e(\xi) \frac{\partial^2 w_e(\xi, t)}{\partial \xi^2} d\xi,
 \tag{10}$$

where the constant K_s is determined by the properties of the piezoelectric material and w_e is the translational displacement of the beam [1, 5]. This displacement is also approximated by the shape functions as

$$w_e(\xi, t) = [N_{e1}(\xi) N_{e2}(\xi) N_{e3}(\xi) N_{e4}(\xi)] \begin{Bmatrix} w_{e1}(t) \\ w_{e2}(t) \\ w_{e3}(t) \\ w_{e4}(t) \end{Bmatrix}.
 \tag{11}$$

Combining equations (8)–(11) gives the sensor output for the element as

$$y_e = \begin{Bmatrix} f_{e1} \\ f_{e2} \\ f_{e3} \\ f_{e4} \end{Bmatrix}^T \mathbf{C}_e \begin{Bmatrix} w_{e1} \\ w_{e2} \\ w_{e3} \\ w_{e4} \end{Bmatrix},
 \tag{12}$$

where the (i, j) th element of the matrix \mathbf{C} is

$$\mathbf{C}_{eij} = K_s \int_0^{\ell_e} N_{ei}(\xi) N_{ej}''(\xi) d\xi,
 \tag{13}$$

giving

$$\mathbf{C}_e = -\frac{K_s}{30\ell_e} \begin{bmatrix} 36 & 33\ell_e & -36 & 3\ell_e \\ 3\ell_e & 4\ell_e^2 & -3\ell_e & -\ell_e^2 \\ -36 & -3\ell_e & 36 & -33\ell_e \\ 3\ell_e & -\ell_e^2 & -3\ell_e & 4\ell_e^2 \end{bmatrix}.
 \tag{14}$$

The sensor output, y , is the sum of the contributions of the elements given by,

$$y = \sum_e y_e = \mathbf{f}^T \mathbf{C}_s \mathbf{q}. \quad (15)$$

Here the element matrices have been assembled into the global matrix \mathbf{C}_s , in the usual way. The element nodal displacements, w_{ei} , have been incorporated into the global displacement vector \mathbf{q} , and the sensor nodal “widths” f_{ei} have been assembled into a global vector \mathbf{f} . However, the sensor nodal widths at the clamped boundary conditions are not set to zero, whereas the corresponding displacements are set to zero. Thus, in general \mathbf{C}_s is a rectangular matrix. Upon comparing equations (1) and (15), it is clear that

$$\mathbf{C}_q = \mathbf{f}^T \mathbf{C}_s \quad (16)$$

and the sensor design changes from finding \mathbf{C}_q as a solution of equation (6) to finding \mathbf{f} as a solution of

$$\mathbf{f}^T \mathbf{C}_s \Phi = \mathbf{C}_p. \quad (17)$$

Thus, the methods introduced earlier may be applied using $\mathbf{C}_s \Phi$ rather than Φ .

The procedure for actuators is very similar. If $f(\xi)$ is now the width of the actuator, then the work done by the actuator is [5]

$$U_e(t) = K_a \int_0^{\ell_e} f_e(\xi) \frac{\partial^2 w_e(\xi, t)}{\partial \xi^2} u(t) d\xi = \begin{Bmatrix} w_{e1} \\ w_{e2} \\ w_{e3} \\ w_{e4} \end{Bmatrix}^T \mathbf{B}_e \begin{Bmatrix} f_{e1} \\ f_{e2} \\ f_{e3} \\ f_{e4} \end{Bmatrix} u(t), \quad (18)$$

where the constant K_a is determined by the properties of the piezoelectric material, and u is the actuator input. The matrix \mathbf{B}_e equals the transpose of \mathbf{C}_e , with K_s replaced by K_a . Assembling the contributions from all the elements gives the force input as

$$\mathbf{B}u = \mathbf{B}_s \mathbf{f}u, \quad (19)$$

where the global matrix \mathbf{B}_s is assembled from the element matrices \mathbf{B}_e . Again the design of modal actuators is similar to before, but instead of computing \mathbf{B} as a solution of equation (4), \mathbf{f} must be computed as a solution of

$$\mathbf{B}_m = \mathbf{M}_m^{-1} \Phi^T \mathbf{B}_s \mathbf{f}. \quad (20)$$

6. MINIMIZING TRANSDUCER CURVATURE

One option to ensure that the transducer may be manufactured as easily as possible is to minimize the curvature of its width. Thus, one wishes to minimize,

$$J = \sum_e \int_0^{\ell_e} f_e''(\xi)^2 d\xi = \sum_e \begin{Bmatrix} f_{e1} \\ f_{e2} \\ f_{e3} \\ f_{e4} \end{Bmatrix}^T \mathbf{H}_e \begin{Bmatrix} f_{e1} \\ f_{e2} \\ f_{e3} \\ f_{e4} \end{Bmatrix} \quad (21)$$

where

$$\mathbf{H}_{eij} = \int_0^{\ell_e} N''_{ei}(\xi) N''_{ej}(\xi) d\xi. \tag{22}$$

\mathbf{H}_e looks like the element stiffness matrix with a unit flexural rigidity. Assembling the contributions from all the elements gives

$$J = \mathbf{f}^T \mathbf{H} \mathbf{f}, \tag{23}$$

where \mathbf{H} contains the element matrices, \mathbf{H}_e , and is symmetric. Consider the sensor design problem. This requires that J is minimized, subject to equation (17). This constrained problem may be solved by using Lagrange multipliers, that is by minimizing

$$J = \mathbf{f}^T \mathbf{H} \mathbf{f} + [\mathbf{f}^T \mathbf{C}_s \Phi - \mathbf{C}_p] \lambda, \tag{24}$$

where λ is a vector of Lagrange multipliers. Differentiating with respect to \mathbf{f} , and setting the result to $\mathbf{0}$, produces the solution as

$$\begin{bmatrix} 2\mathbf{H} & \mathbf{C}_s \Phi \\ \Phi^T \mathbf{C}_s^T & \mathbf{0} \end{bmatrix} \begin{Bmatrix} \mathbf{f} \\ \lambda \end{Bmatrix} = \begin{Bmatrix} \mathbf{0} \\ \mathbf{C}_p^T \end{Bmatrix}. \tag{25}$$

Note that equation (25) may be ill-conditioned and the matrix rank deficient. In this case, the solution is obtained by using the Moore–Penrose pseudo-inverse. A similar solution may be obtained for the actuator.

7. THE BEAM EXAMPLE REVISITED

The beam example described earlier will now be used to design a distributed sensor. It is assumed that beam is excited at node 7 by a translational force input. The sensor gain constant is assumed to be unity, $K_s = 1$, since it is most important to compute the sensor shape, rather than the calibration constant. Figure 5 shows the shape of the sensor designed

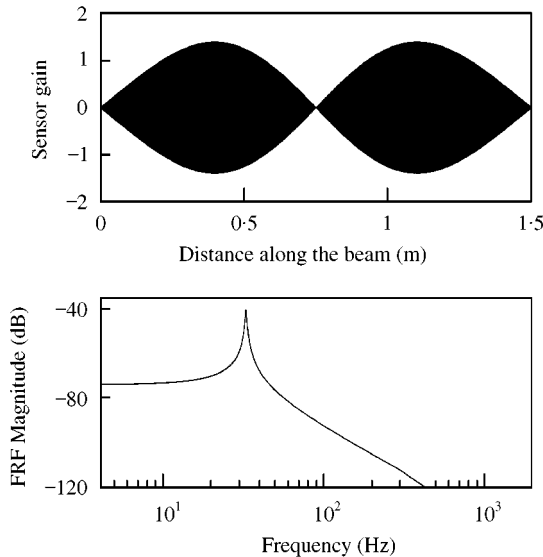


Figure 5. The distributed sensor shape and receptance designed to excite the second mode.

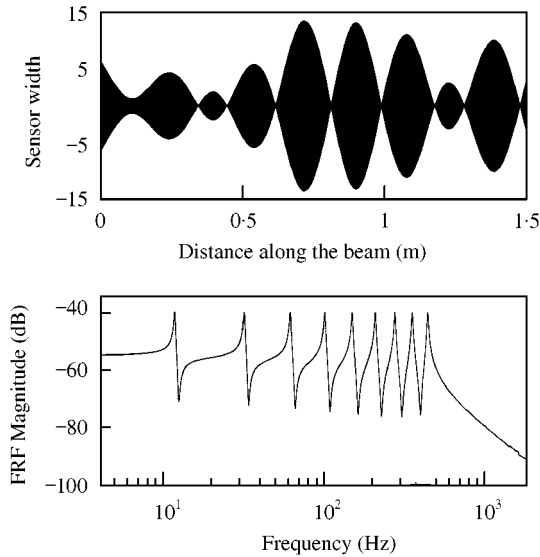


Figure 6. The distributed sensor shape and receptance designed to excite the first nine modes equally.

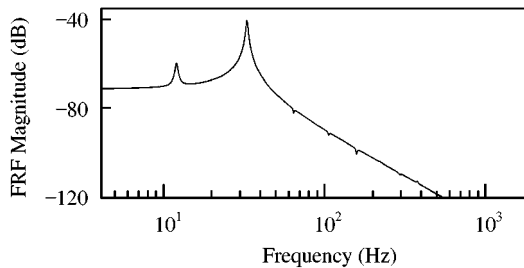


Figure 7. The errors introduced by non-proportional damping.

to excite only the second mode, with a peak in the receptance of 0.01 m/N . Again nine modes are assumed to be of interest. The shape was obtained from equation (25), and the nodal width values used, together with the element shape functions, to produce a continuous sensor width function. Clearly, the shape is very much like the second mode of the beam. Figure 6 shows the sensor design when all nine modes are excited, with all their peak receptance magnitude at 0.01 m/N . Notice that the sensor shape is now very complicated. Also the sensor is not symmetric because the beam is not excited at the centre.

The transducer design has been formulated under the assumption of proportional damping, where the undamped modes are able to diagonalize the damping matrix, as well as the mass and stiffness matrices. Suppose a discrete, grounded, translational damper with coefficient 1 Ns/m is added to the beam at node 10. This produces non-proportional damping, and changes the damping ratios of the first two modes to 1.87% and 1.43% , from the 1% without the damper. The damping ratios of the higher modes are changed, but less significantly, yielding damping ratios between 1 and 1.08% . Figure 7 shows the receptance of the beam

using the sensor designed by assuming proportional damping to excite the second mode only. The actual damping ratio of 1.43% was used to determine the maximum magnitude of the second mode, and to ensure it equals 0.01 m/N. It is clear that the first mode is excited significantly, and the higher modes are excited to a lesser extent. Although it may be possible to design discrete modal sensors for non-proportionally damped systems, for distributed sensors designed by varying the width, one inherently assumes that the modes are real. Therefore, the errors introduced by non-proportional damping cannot be removed.

8. CONCLUSIONS

This paper has considered the problem of designing modal actuators and sensors using a discrete approximation to the equations of motion. For discrete sensors the redundancy in the modal filtering requirements has been used to introduce side constraints on the transducer gains. These constraints may reduce the number of transducers by using only a subset of them, or may ensure orthogonality to higher modes. The second approach is for distributed transducers for arbitrary beam-type structures, where the transducers are approximated by using the underlying finite element shape functions. This allows the actuators and sensors to be designed by using the discrete approximation and the shape recovered by using the shape functions. The side constraint in this case was the minimization of the curvature of the transducer, although constraints requiring the transducer to cover only part of the structure are also possible. This approach gives the possibility of designing modal transducers for more general structures modelled by using finite element analysis.

ACKNOWLEDGMENTS

Dr Friswell gratefully acknowledges the support of the Engineering and Physical Sciences Research Council through the award of an Advanced Fellowship.

REFERENCES

1. C.-K. LEE and F. C. MOON 1990 *ASME Journal of Applied Mechanics* **57**, 434–441. Modal sensors/actuators.
2. R. L. CLARK and S. E. BURKE 1996 *ASME Journal of Vibration and Acoustics* **118**, 668–675. Practical limitations in achieving shaped modal sensors with induced strain materials.
3. N. TANAKA, S. D. SYNDER and C. H. HANSEN 1996 *ASME Journal of Vibration and Acoustics* **118**, 630–640. Distributed parameter modal filtering using smart sensors.
4. Y. ZHUANG and J. S. BARAS 1994 *Smart Structures and Intelligent Systems, Proceedings of SPIE* **2190**, 381–388. Shape optimisation of distributed sensors and actuators for smart structure control.
5. C.-Y. HSU, C.-C. LIN and L. GAUL 1998 *Smart Materials and Structures* **7**, 446–455. Vibration and sound radiation controls of beams using layered modal sensors and actuators.
6. M. I. FRISWELL 1999 *Journal of Vibration and Control* **5**, 619–637. Partial and segmented modal sensors for beam structures.
7. W. GAWRONSKI 2000 *Journal of Sound and Vibration* **229**, 1013–1022. Modal actuators and sensors.
8. P. C. HUGHES and R. E. SKELTON 1980 *ASME Journal of Applied Mechanics* **47**, 415–420. Controllability and observability of linear matrix-second-order systems.
9. J. J. DOSCH, D. J. INMAN and E. GARCIA 1992 *Journal of Intelligent Material Systems and Structures* **3**, 166–185. A self sensing piezoelectric actuator for collocated control.

10. A. J. MILLAR 1990 *Subset Selection in Regression*. Monographs on Statistics and Applied Probability **40**, London: Chapman & Hall.
11. M. I. FRISWELL, J. E. MOTTERSHEAD and H. AHMADIAN 1998 *ASME Journal of Vibration and Acoustics* **120**, 854–859. Combining subset selection and parameter constraints in model updating.
12. L. MEIROVITCH 1990 *Dynamics and Control of Structures*. New York: John Wiley & Sons.